www.czasopisma.pan.pl PAN www.journals.pan.pl

Opto-Electronics Review 25 (2017) 110–117

Contents lists available at ScienceDirect

Opto-Electronics Review

journal homepage: http://www.journals.elsevier.com/opto-electronics review

Estimation and correction of the influence of an IR spectometer on mechanical vibrations

R. Pietrzak*, M. Rataj*

Space Research Centre, Polish Academy of Science, ul. Bartycka 18A, 00-716 Warsaw, Poland

ARTICLE INFO

Article history:
Received 16 January 2017
Received in revised form 24 March 2017
Accepted 9 April 2017
Available online 20 April 2017

Keywords:
Fourier spectroscopy
Vibrations

ABSTRACT

The problem of influence of mechanical vibrations on a measurement is well known and analyzed for ground conditions. However, the problem becomes quite essential and difficult to solve in space conditions. The influence of vibrations on accuracy of the measurement was observed on MIPAS – ENVISAT and in PFS Mars Express.

This paper presents an experimental and theoretical investigation on sensitivity to mechanical disturbances of the Fourier-transform infrared spectrometer PFS.

A theoretical analysis has been performed in order to highlight the expected effect of the vibration, then laboratory tests have been designed and carried out for instrument characterization.

The theoretical investigation has been confirmed by experimental tests.

The data were distorted by errors that reflect the influence of vibrations on the instrument and temperature instability of the reference source.

The considerations are a perfect example presenting the scale of vibrations problem and the instability of the reference source in assessing accuracy of the measurement in space.

1. Introduction

This paper presents an experimental and theoretical investigation on sensitivity of a Fourier-transform infrared spectrometer to mechanical disturbances. The problem has been observed in many space missions, especially in MIPAS – ENVISAT and PFS – MARS EXPRESS instruments.

In the paper, the theoretical and experimental considerations were referred to general disturbances in Fourier spectrometers coming from spacecraft vibrations even when it does not have an important influence on recalled instruments.

A basic optical layout of the Fourier spectrometer, which is based on the Michelson interferometer, is illustrated in Fig. 1. The incident beam from the source S is collimated by the parabolic mirror C and divided by the beam splitter B into two parts: the reflected beam that travels to a fixed mirror M_2 and back, and the transmitted beam's travel to a moving mirror M_1 and back. The parabolic mirror R focuses an interference beam to the detector D.

The output intensity of the interferometer for a monochromatic source is written as [1]:

$$I(z,\sigma) = I_1(\sigma) + I_2(\sigma) + 2\sqrt{I_1(\sigma)I_2(\sigma)}\cos(2\pi\sigma z) \tag{1.1}$$

where:

$I(z,\sigma)$ – measured signal,

$I_1(\sigma), I_2(\sigma)$ – intensity of both beams, for different wave number (σ),

σ – wave number,

$z = 2d$ – path difference.

The measured signal acts simultaneously with the reference signal (usually a laser diode signal) within the global system. The reference signal plays the role of a trigger for measurements.

The total signal – interferogram (1.1) from the whole spectral band is:

$$R(z) = \int_{-\infty}^{\infty} I(z,\sigma)\,d\sigma \tag{1.2}$$

The Fourier transform of the interferogram can be written as [1]:

$$FT^{-2\pi\sigma x}[R(z)] = C\delta(\sigma) + f(-\sigma) + f(\sigma) \tag{1.3}$$

where, C – constant; $\delta(\sigma)$ – Dirac delta function; $f(-\sigma)$, $f(\sigma)$ – the function depends on the intensity of radiation, the spectral sensitiv-

* Corresponding authors.
E-mail address: robertp@cbk.waw.pl (R. Pietrzak).

http://dx.doi.org/10.1016/j.opelre.2017.04.003
1896-3757/

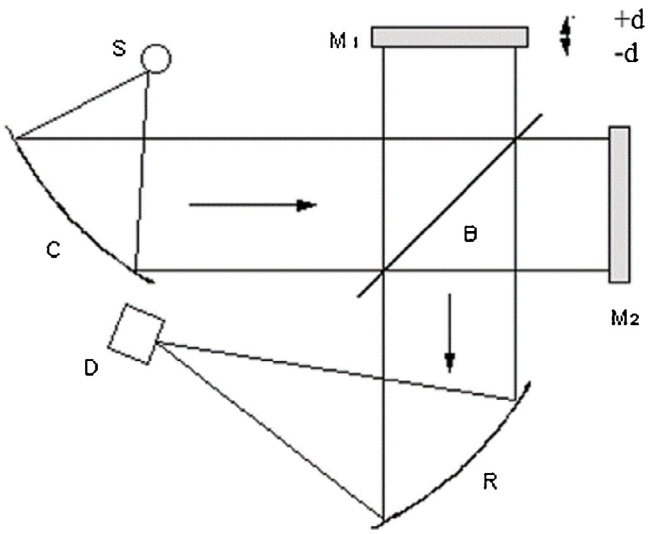

Fig. 1. The Michelson interferometer.

ity of the detector and transmittance coefficients for both branches of the interferometer.

The Fourier transformation of the measured interferogram allows to extract from (1.3) information about spectral characteristics of radiation, the spectral sensitivity of the detector and the transmittance coefficients for both branches of the interferometer.

The measured signal (1.1) can be distorted by many factors. The signal distortions presented in the further parts of the paper are quite good corrected in earthly conditions but the instrument's work in the space is disturbed by many additional factors. They should be considered in the process of calibration and data correction.

The dates (in the space) are distorted (modulated) because of a vibration of the satellite (despite the muffler). These distortions were not observed during tests in laboratory.

In general, many sources of a vibration are expected for an orbiting spacecraft. They have origin from:

- the main engine and the attitude control thrusters,
- the reaction wheels which are active all the time during scientific observations,
- the inertial measuring units include dithered ring laser gyros, dither actuators producing nearly always present harmonic vibrations,
- solar panels: their orientation may be continuously changed to a point toward the Sun during scientific data acquisition.

The observed errors are directly linked to the amplitude and phase of the recorded signal.

They are transferred to the recorded signal by sampling arrangement (amplitude modulation and phase modulation of the reference source), vibration of the mirror, detector (through amplitude modulation) and nonlinearities in detector + amplifier + analogue to the digital converter system (intermodulation).

In this paper, we will focus on an analysis of the signal errors are of a periodic amplitude and phase modulation, resulting from the described above vibrations of the device. A theoretical description of the arising errors and new methods for their correction will be presented. The theoretical considerations to data from the PFS and laboratory Fourier spectrometer on which we executed the simulation described above modulations will be brought back.

The introduced algorithms of the phase and amplitude correction of the recorded signal constitute new approach to the case of this type error correction. The advantage of the method is that the modulation parameters are marked from the reference signal which is a single spectral line.

2. Theoretical analysis of an errors in the reference and measured signal

These errors can be divided into three types:

- amplitude modulation,
- phase modulation,
- intermodulation errors of the measured signal.

The amplitude modulation and phase modulation of a reference signal are conducted respectively using the same reference signal. However, the amplitude modulation of a reference signal comes from modulation of cosine function but phase modulation exists as argument of cosine function.

The correction methods were divided into two parts due to provide better reproducibility of the original signal. However, correction methods are based on an automatic identification of the different type of error and can be easy implemented to a single tool [2].

The presented above signal modulations can be written as:

• Amplitude modulation

$$I_{AM}(z) = I(z)\left[1 + \varepsilon_p(z)\right] \tag{2.1}$$

where:
$I_{AM}(z)$ – modulated signal,
$I(z) = R(z, \sigma)$ – measured signal,
$\varepsilon_p(z) = \varepsilon_r(z) + \varepsilon_i(z)$ – error of the signal,
$\varepsilon_r(z)$ – real part of the error,
$\varepsilon_i(z)$ – imaginary part of the error.
z – path difference.

For a periodic amplitude modulation two additional lines "twins" σ_{01} and σ_{02}, for every spectral feature are created. Since both spectral lines are symmetric: $\sigma_{02} - \sigma_0 = \sigma_0 - \sigma_{01}$, and $\varepsilon_i(z) = 0$, the signal errors can be described as: $\varepsilon_p(z) = \varepsilon_r(z) = 2b/a \cos[2\pi(\sigma_{02} - \sigma_0)z]$,
where:
σ_0 – wave number of the central line,
σ_{02}, σ_{01} – wave numbers of the side spectral lines,
$m = 2b/a$ – depth of modulation.

• Phase modulation

Modulated signal can be written as:

$$I_{PM}(z) = I[z + \varepsilon_p(z)] \tag{2.2}$$

Because $\varepsilon_r(z) = 0$ for phase modulation $\Rightarrow$ $\varepsilon_p(z) = \varepsilon_i(z) = (2b/a)\sin[2\pi(\sigma_{02} - \sigma_0)z]m\sin(2\pi Fz) \Rightarrow F = (\sigma_{02} - \sigma 0)$. For phase modulation the phase of the measured signal $I_{PM}(z)$ is variable as opposed to amplitude modulation, where the phase is constant. The F is defined also in the frequency area as $F_d = Fv$ and will be used in the further part of the paper, v – is the velocity of mirror.

• Intermodulation errors of the signal

$$I_{Im}(z) = I(z) + \alpha I^2(z) + \beta I^3(z) \tag{2.3}$$

α, β – coefficients of the transfer function.

This modulation is related to the nonlinearity of the detector and the consideration will be limited to the first and the second

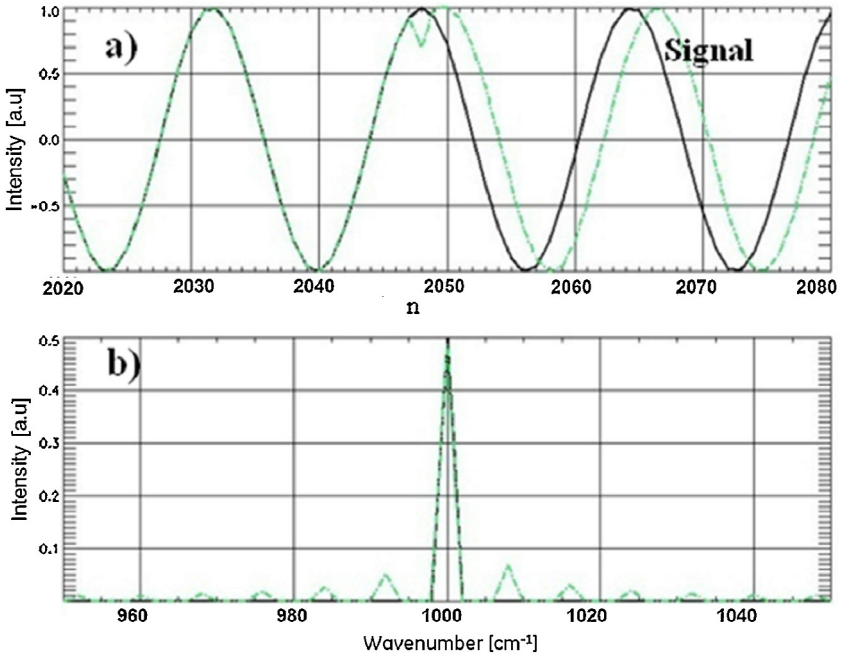

Fig. 2. Single line (a) and spectrum (b) (black line – before extra sampling, green line –after extra sampling), n – sample number.

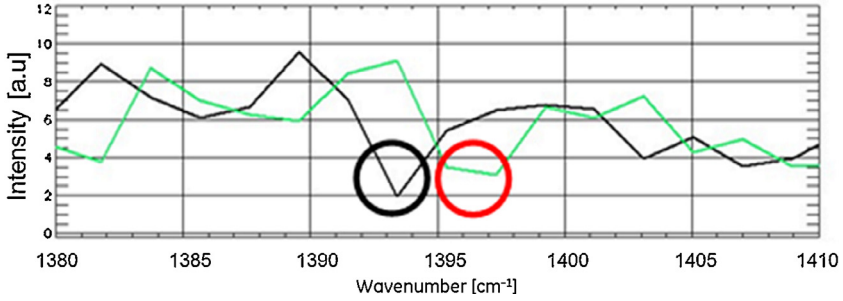

Fig. 3. The synthetic line of the atmosphere 1393.6 cm^{-1} (black line), with extra sampling (green line) 1397 $cm-^{1}$.

power of error. The theoretical consideration and proposed correction methods of amplitude and phase modulation will be presented in the next parts of paper. The paper has been divided into the parts related to amplitude modulation of reference and detected signal with correction methods. As well as the analogue part dedicated to phase modulation.

2.1. Amplitude modulation of the reference signal – theoretical analysis

The configuration of the instrument, with the sampling based on the signal of a reference laser, is the one that minimizes the effects of mechanical vibrations being in principle based on a constant optical path sampling strategy because a monochromatic laser traveling in the optical system of the incoming IR beam, generates a reference interferogram (ideally a cosine function). An electronic circuit generates a trigger signal from each zero crossing of the reference interferogram, corresponding to an optical path change of half the laser wavelength [3]. This control system shall be insensitive to the external distortion and interferometer mirrors speed changes. However, even in this situation optical path intervals between samplings can be different due to modulations of the reference signal. It can be demonstrated as offsets (amplitude modulation) and delays (phase modulation) in the reference signal [1,4].

It shall be noticed that even if the interferogram was sampled at constant OPD another effect of velocity changes would take place because of the nonconstant time step (filtering the signal in the frequency domain instead of wavenumber).

Per Eq. (2.1) the reference signal is:

$$I_{AM}(z) = I_0(z)\, a\, \cos(2\pi\sigma_0 z)\left\{1 + m\, \cos[2\pi F z]\right\} \tag{2.4}$$

and after transformation:

$$I_{AM}(z) = I_0(z)\, a\left\{\cos(2\pi\sigma_0 z) + \frac{m}{2}\cos[2\pi z(\sigma_0 - \sigma_{02})] + \frac{m}{2}\cos[2\pi z(\sigma_{02})]\right\} \tag{2.5}$$

where:

a – amplitude of the central line (see Fig. 2),

b – amplitude of side spectral lines: σ_{01} and σ_{02} (see Fig. 2),

$I_0(z)$ – constant value of the interferogram.

The main conditions of reference signal modulation are described below.

If $0 < m < 1$ the overmodulation does not interfere. If $m \geq 1$ the overmodulation signal is received.

From Eq. (2.4) we can see, that if:

$$a > 2b \Rightarrow m < 1 \Rightarrow N_x \equiv 0$$

$$a = 2b \Rightarrow m = 1 \Rightarrow N_x \equiv (\sigma_{01} - \sigma_0) z_{\max}$$

$$a < 2b \Rightarrow m > 1 \Rightarrow N_x \equiv 2(\sigma_{01} - \sigma_0) z_{\max}$$

z_{max} – maximum path difference,

N_x – extra sampling points defined by above relationships.

If $m < 1$ the amplitude modulation of the reference signal does not introduce additional signal errors, because there are no additional sampling points in the signal.

In the second and third case ($a = 2b$, $a < 2b$) additional sampling points in the modulation signal are generated. For $m = 1$, additional samples can be generated for the frequency which are even with the frequency of the modulation wave. The extra sampling points cause a shift to the right from the correct interferogram vector with regard to the extra point itself.

In the last case, oversampling follow. Additional samples become generated with the frequency equal to $2\sigma_0$. If $m > 1$, in every two additional samples that are in the distance equal to the period of the reference signal and the correct interferogram is shifting to the right about two extra points.

The process is similar in all cases: following the generation of additional spectral lines around the main line, depending on the frequencies of the modulation and the kind of extra sampling. The shift of the main spectral line after the modulation process in relation to the line before the modulation can be additionally noticed.

Extra sampling generates additional harmonics and produces a shift in the frequency domain.

Fig. 3 shows the synthetic line of the atmosphere 1393.6 cm^{-1} (black line), with extra sampling (green line) 1397 cm^{-1}. The spectrum is shifted in the frequency range and distorted because of generating additional spectral lines.

The extra sampling points in the continuous spectrum, like in the case of a single line, shift every line in frequency range, together with the generation of additional frequencies. Amplitude of additional spectral lines can reach about 15% of the maximum of the central line. The influence of oversampling of the laser source on the measured signal introduces considerably larger errors. Consequently, it can lead to a wrong interpretation.

The measured spectrum (a) and the simulation spectrum (b) for modulated parameters: $F_d = 205$ Hz, $m = 1$ are on the Fig. 4.

A similar shift of the individual spectral lines and the analogous change of their shape show that both spectra were distorted similarly. The red line is the spectrum with the amplitude modulation

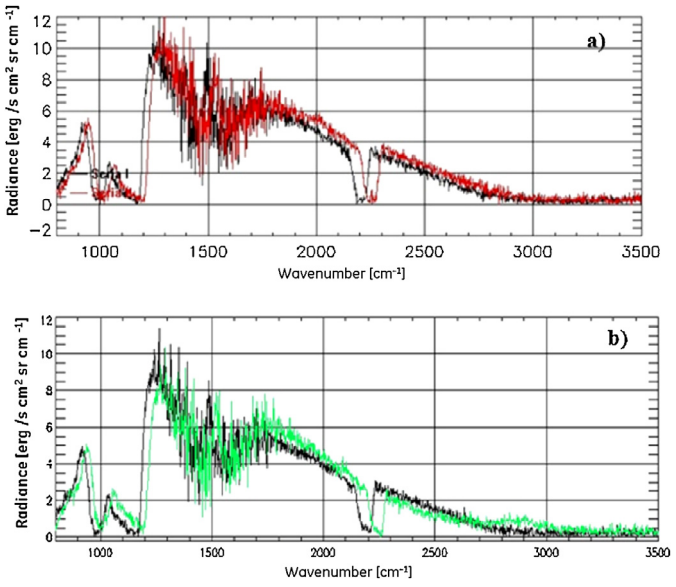

Fig. 4. Atmospheric spectrum, black line – spectrum before modulation, green line (synthetic spectrum) and red line (real spectrum after overmodulation), $F_d = 205$ Hz, m = 1.

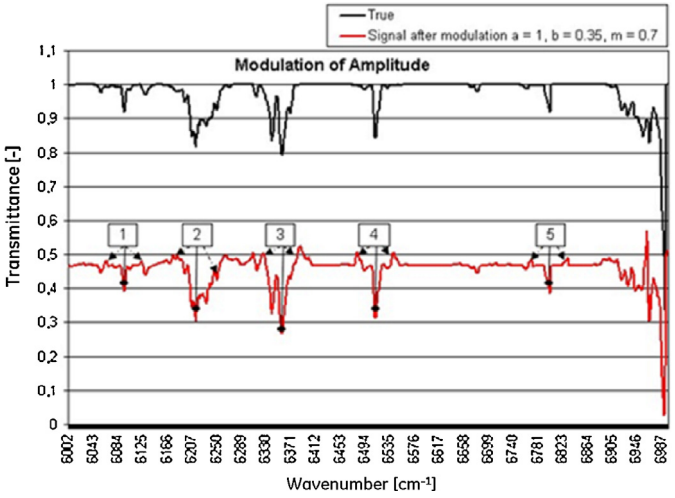

Fig. 5. The example of the spectrum modulation CO_2 for different parameters a and b, $m = 0.7$.

with $F_d = 205$ Hz and the green line is the synthetic spectrum with the amplitude modulation.

2.2. *Amplitude modulation of the measured signal – theoretical analysis*

The modulation of the measured signal generally comes from the cyclic misalignment [3] and mirror vibrations [3,4]. This kind of errors can be expressed as:

$$I_{AM}(z, \sigma) = I(z, \sigma)[1 + m\cos(2\pi Fz)] \tag{2.6}$$

where:

$I(z, \sigma)$ – measured signal.

Fig. 5 shows the synthetic spectrum of CO_2 with amplitude modulation.

The amplitude modulation of the measured signal creates two additional lines ("twins") of every spectral feature (for $\sigma_{0mod} = \sigma_0 \pm \sigma_{mod}$) on the spectrum, σ_{0mod} – the wave numbers of spurious lines generated by the disturbance, σ_{mod} – the equivalent in wave number of the frequency of the disturbance (the numbers 1...5 mark the wave numbers of the spurious lines) (Fig. 5). The decreasing of the signal level is visible and the power has been passed to the side lobes.

$$P_y = \frac{1}{2}A_o\left(1 + \frac{m^2}{2}\right) \tag{2.7}$$

The analogous effect is observed when the real continuous spectrum is analyzed.

The atmosphere spectrum with amplitude modulation yielding spurious lines generated by the disturbance has been shown in Fig. 6.

In this paper the amplitude modulation errors are identified and discussed. The amplitude modulation produces sidebands located symmetrically on both sides of each spectral feature (at $\pm\sigma_{mod}$) and changes the spectrum intensity. The shift of the spectral line does not appear.

Additionally, the amplitude modulations of the reference signal (extra sampling) produce a displacement of the reference signal.

2.3. Correction of the spectrum with amplitude errors

The correction of the spectrum with reference source amplitude errors is executed in two steps:

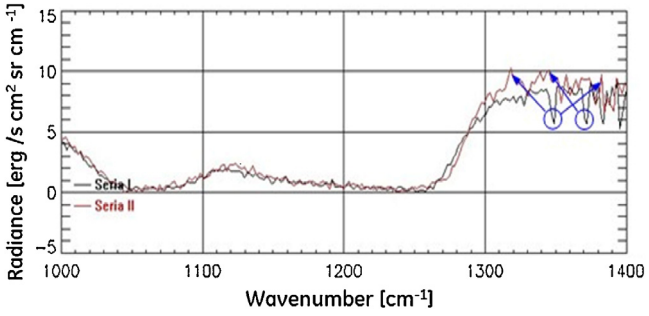

Fig. 6. The atmospheric spectrum, black line – spectrum before modulation, red line – spectrum after modulation F_d = 60 Hz.

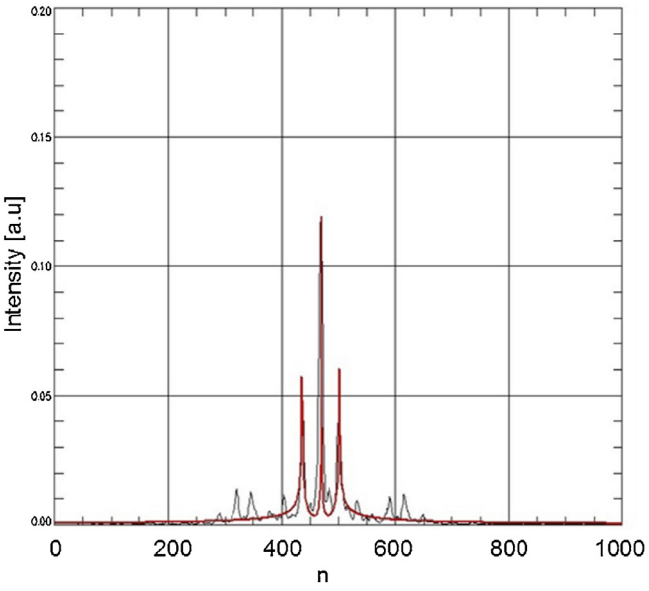

Fig. 7. The spectrum of the laser for PFS – SWC (black line), red line – the approximation function (n – sample number).

- **Defining the parameters of the modulation reference signal: *m*, *F***

For harmonic sampling errors $\varepsilon_p(z)$, the interferogram is constructed by using Eq (2.5).

The parameters: m and F of modulation can be defined by a minimization function [2,4] between modulated signal and ideal signal (without amplitude modulation $I(z)$).

The laser spectrum for SW – Planetary Fourier Spectrometer (black line) and the approximation function are shown in Fig. 7.

In this case the applied method fits the modulation signal to second harmonic with an arbitrary error of about 0.02. This method does not reproduce the side lines (above the second). Moreover, the power of the side harmonics is low (about 0.1 of the central line), so they can be neglected.

- **Correction of the spectrum with amplitude errors**

The amplitude modulation of the signal is written as: (2.5). We can define the vector $I(z,\sigma)$ (signal without modulation) from (2.6) when F and m are known. The parameters F and m were calculated per the foregoing method.

The spectrum before and after amplitude correction is presented in Fig. 8.

The maximum relative different between ideal spectrum and modulated after recovery can be corrected with an accuracy of about 5%. Based on the experiences [2] and good practice, this accuracy does not introduce problems of spectral lines identification.

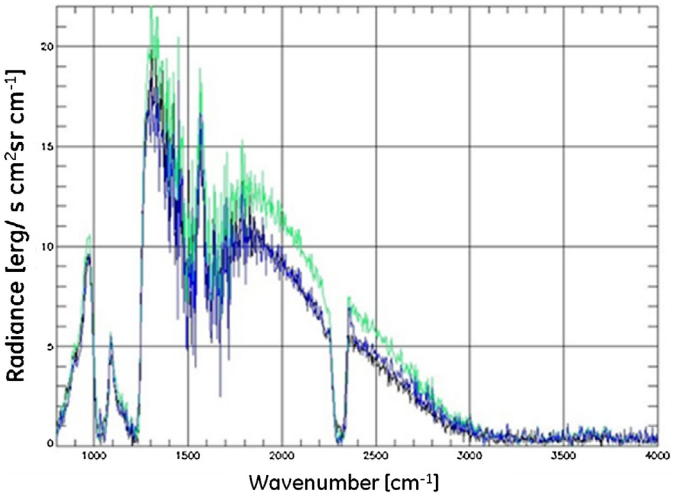

Fig. 8. Atmospheric spectrum, black line – spectrum before modulation, blue line – corrected spectrum, green line – spectrum after amplitude modulation, for F_d = 205 Hz, m = 0.5.

The exact depth and frequency of the modulation is very important for a proper correction. It is possible due to a good fitting of the reference signal to the measured signal.

The deficiency of the introduced method consists of the considerable time of calculations.

The correction of the extra sampling can be realized similarly to the correction of the errors with phase modulation of the reference signal. This topic is described in details in the next chapter.

2.4. Phase modulation of the reference signal – theoretical analysis

A stable temperature of the laser in Fourier spectroscopy produces a distortion of the basic spectral line.

The interferogram $I_{PM}(z)$ has been given by Eq. (2.2) for harmonic sampling errors $\varepsilon(z)$.

The Taylor expansion of $I_{PM}(z)$ is used and truncated after the third term:

$$I_{PM}(z) = \left\{ I(z) + I'(z)\varepsilon_p(z) + 0.5I''(z)\varepsilon_p^2(z) \right\} \tag{2.8}$$

Assumed harmonic phase errors:

$$\varepsilon_p(z) = m\ \sin(2\pi Fz) \tag{2.9}$$

The interferogram can be expressed in terms of Bessel functions:

$$I_{PM}(z) = I_o(z) \sum_{m=-\infty}^{\infty} J_m(m) \cos\{2\pi z(\sigma_o + nF)\} \tag{2.10}$$

Where:

n – order of the modulation,

$I_o(z)$ – constant value of the interferogram.

The spectrum can be expressed as:

$$S_{PM}(L) = 0.5I_o(\sigma_o) \sum_{m=-\infty}^{\infty} J_m(m)\{\delta(\sigma - \sigma_o - nF) + \delta(\sigma + \sigma_o + nF)\} \tag{2.11}$$

where:

σ – wave number of the band,

σ_o – wave number of the central line.

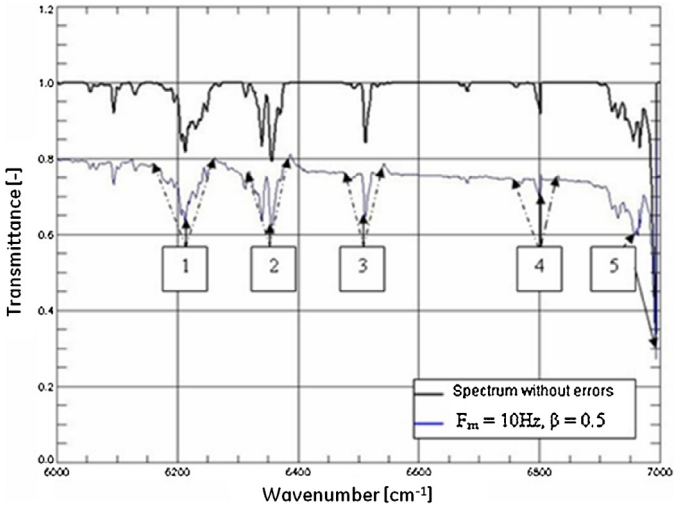

Fig. 9. The phase modulation of the synthetic line CO_2, $F_d = 10$ Hz, $m = 0.5$.

The relative amplitude of the "ghosts" is roughly equal to the sampling error expressed as a fraction of the sampling step: $m\sigma_0\Delta$, where Δ is the sampling step. It can be said that the amplitude of the next harmonic is equal to the Bessel function, whose order depends on the number of harmonic.

The phase modulation of the reference signal generates many spectral lines of various amplitudes. The spectrum contains the central line and infinitely many pairs of sidelines, which are spaced by $\pm F, \pm 2F, \ldots$ from the central line. The amplitude of the central line is defined by the Bessel function of order zero. The successive orders of Bessel functions define higher order of the amplitude.

"Orphan ghosts" are observed in the spectrum, these are ghosts arising from spectral lines laying outside the observed spectrum.

In the first case when "ghosts" are together with the "mother spectral" there are quite easy to identify.

However, in the second case when "ghosts" come from lines, which are outside the spectral band, they create a quite essential problem with identifying and they are the cause of huge errors in the observed spectra.

It should be stressed, for all spectral lines anti symmetric lines are generated.

An example of the phase modulation is presented below. The ideal synthetic CO_2 line and a modulated line with modulation parameters: $F_d = 10$ Hz, $m = 0.5$ can be seen.

The spectral CO_2 line (black line) was modulated per the (2.9) (blue line) (Fig. 9).

Phase errors have sinusoidal form: $\varepsilon_p(z) = m\Delta \sin 2\pi\sigma_0 z$, where Δ – is the sampling interval, m – depth of the modulation. The FT of this function is an anti-symmetric pair of delta functions with amplitude: $m\Delta/2$.

2.5. Correction of the spectrum with phase errors of the reference source

The correction of the spectrum with phase errors of the reference source is carried on in two steps:

- **Defining the parameters of the modulation reference signal *m*, *F***

For harmonic sampling errors $\varepsilon_p(z)$, the interferogram is obtained using Eq. (2.2). The definition parameters of the phase modulation are similar to the case of amplitude modulation. Fig. 10 gives the example of defining the modulation signal parameters m, F for the PFS laser.

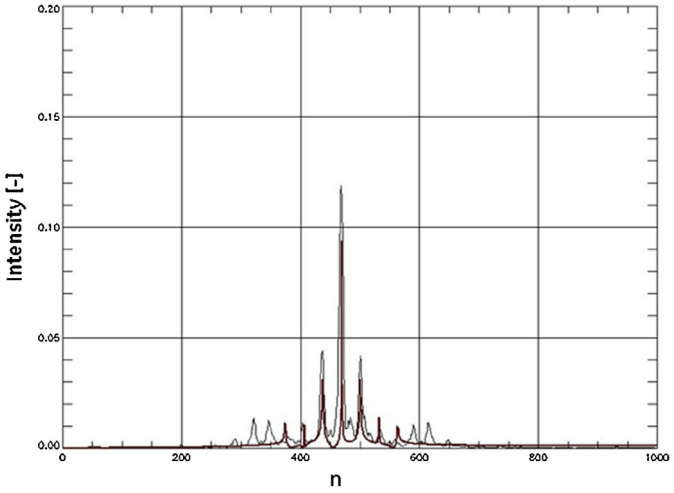

Fig. 10. Spectrum of the laser for PFS – SWC (black line) with the approximation function (brown line).

Parameters for the laser spectrum of the PFS were calculated by means of a minimization method [5]:

- The central wave: 2000 cm^{-1}
- The modulation wave: 20 cm^{-1}
- The coefficient of the modulation: 1.

- **Correction of the spectrum with phase errors of the reference source**

Using the Taylor series Eq. (2.8) can be written as:

$$I_{PM}(z) = \{I(z) + I'(z)\varepsilon_p(z) + 0.5I''(z)\varepsilon_p^2(z) \tag{2.12}$$

Per the general properties of the Fourier transform:

$I^{(n)}(z) = DT\{(2\pi i\sigma)^n DT[I(z)]\}$, DT – discrete Fourier transform, n – the order of derivative.

Eq. (2.12) can be written as:

$$I_{PM}(z) = \left\{I(z) + [DT(2\pi i\sigma)] \otimes I(z)\right\} \varepsilon_p(z) + 0.5\left\{[DT(2\pi i\sigma)^2] \otimes I(z)\right\} \varepsilon_p^2(z) \tag{2.13}$$

According to [6] Eq. (2.13) can be written in a vector form as:

$$\{I_B\} = \left\{[\bar{I}]^{\mathrm{T}}\{h\}\{\varepsilon_p\} + 0.5[\bar{I}]^{\mathrm{T}}\{h^2\}\{\varepsilon_p^2\}\right\} \tag{2.14}$$

where:

$\{I_B\}$ $I_{PM}(z)$ – is the vector of the function with error,

$[\bar{I}]^{\mathrm{T}}$ – is the transposed matrix (*),

$\{h\} = DT(2\pi i\sigma)$,

$\{\varepsilon_p\}$ – is the vector of the error.

The vector $\{I\}$ (signal without modulation) can be determined from the above equation, when $\{I_B\}$ is known.

Fig. 11 shows the empirical atmospheric spectrum (2000–8000 cm^{-1}) with phase modulation (blue line) and corrected (red line).

The adaptive correction method of the amplitude and phase modulation is characterized by a very good ability to retrieve the raw signal with relative errors ≤ than 4%. High density of the step calculation is required to achieve a minimization of errors.[1]

[1] $^*[\bar{I}]^T \begin{bmatrix} I(0) & I(-1)\ldots & I(-N+1) \\ I(1) & I(0)\ldots & I(-N+2) \\ I(2) & I(1)\ldots & I(-N+3) \end{bmatrix}$.

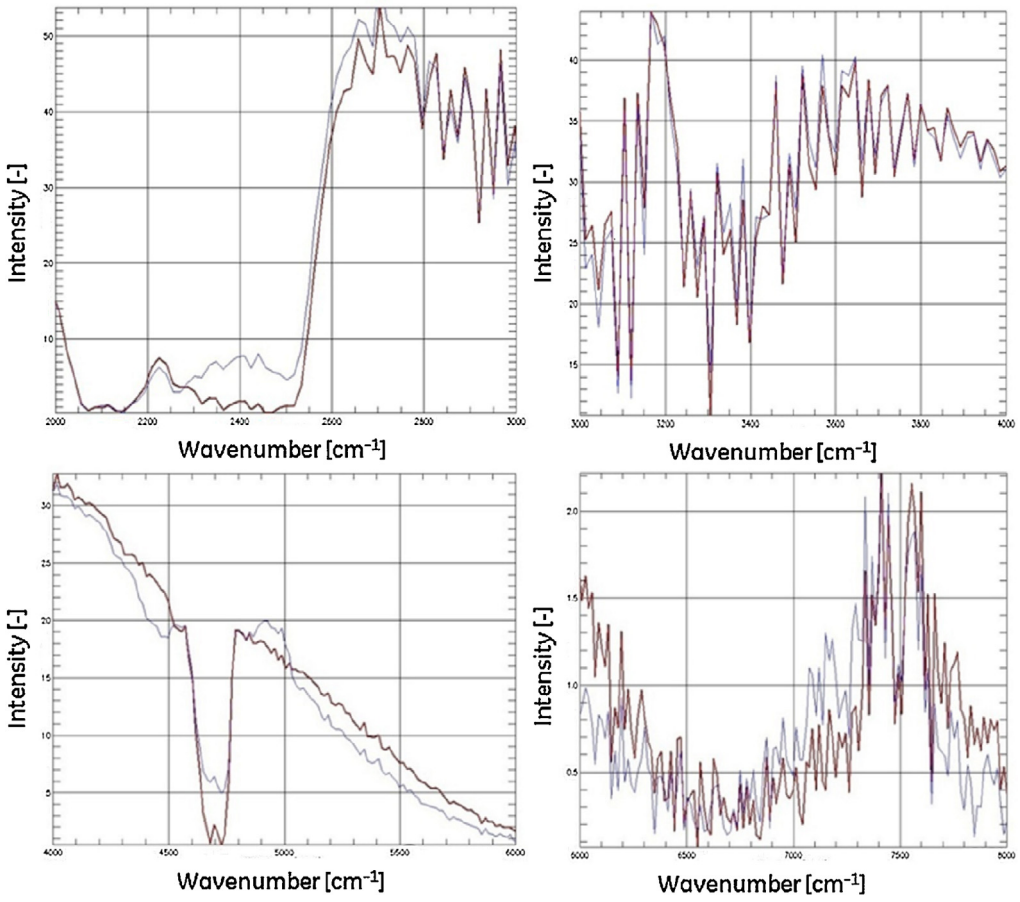

Fig. 11. The atmospheric spectrum after phase modulation (blue line), F_d = 205 Hz, m = 0.5, spectral line after the correction (red line), and black line – spectrum before the phase modulation.

The proposed method of adaptive correction for the amplitude and phase modulation represents a new approach in dealing with errors of this type.

The advantage of the method: the parameters of modulation are obtained from the reference signal which is a single spectral line (this allows qualifying the standard signal easily and the necessity of averaging a few signals and comparing them with the studied signal [2] can be avoided).

However, this method requires the accessibility to the reference signal (which is impossible in some cases). Therefore, guideline for the data acquisition system of Fourier spectrometers in space is the availability of a reference signal.

3. Conclusions

The effect of the random mechanical vibrations on a FTIR spectrometer is negligible (the standard practice is to use the average of several measured signals due to eliminate random errors [2,7]). The main problem appears when the vibration becomes harmonic and errors of the reference signal become periodical. In that case the modulation creates in the spectrum two “twins” of each spectral feature that are similar to the latter but “shifted” in frequency by a quantity corresponding to the frequency of the disturbance. These lines can be wrongly interpreted as real lines.

The effect of mechanical vibrations has large influence on the reference source and on the measured signal. It becomes very important when coefficients of the modulation are larger than unity. Then extra sampling will show up if the sum of amplitudes of sidelines in the laser spectrum is larger than the amplitude of the central line. A shift of the main line in the domain of the frequency range can also be noticed.

This can be seen when the temperature of the reference source varies.

The modulation creates a lot of “twins” of each spectral feature, with an amplitude described by the Bessel function.

References

[1] L. Wawrzyniuk, Analysis of aberrations impact of the optical Fourier spectrometer for the measurement accuracy, Warsaw (Ph.D. dissertation), 1999 (in Polish).
[2] L. Wawrzyniuk, R. Jozwicki, G. Szymanski, M. Rataj, M.I. Blecka, A. Cichocki, R. Pietrzak, Compact dual-band FTIR spectrometer for atmosphere monitoring, Opto-Electron. Rev. 23 (3) (2015) 208–213.
[3] L. Comolli, B. Saggin, Evaluation of the sensitivity to mechanical vibrations of an IR Fourier Spectrometer, Appl. Opt. 46 (2007) 5248–5257.
[4] W. Kimmig, C.E. Blom, Real and imaginary ghosts: a complex correction for interferograms with large sampling errors, J. Atmos. Chem. 30 (1998) 81–101.
[5] J. Szabatin, K. Radecki, Theory of Signals and Modulation, 2nd edn, WPW, Warsaw, 2005 (in Polish).
[6] P. Tomasz, Zieliński, Digital Signal Processing. From Theory to Applications, 2nd edn, WKŁ, Warsaw, 2009 (in Polish).
[7] A.S. Zachor, Drive nonlinearities: their effects in Fourier spectroscopy, Appl. Opt. 16 (1977) 1412–1424.

Robert Pietrzak received his M.Sc. degree in optical engineering at the Precision Mechanics Faculty of Warsaw Technical University in 2008. Currently working toward the Ph.D. degree in Fourier Spectroscopy at Space Research Centre PAS focusing his interest on influence of the amplitude – phase errors on Fourier spectrometer measurement.

Mirosław Rataj received D.Sc. degree in optical engineering (OE) in 2015 at the Mechatronics of Warsaw University of Technology. Working in Space Research Centre PAS since 1984. He is specialization design of spectro-imaging instruments for remote sensing measurements. He was responsible for the design and project management of modules satellite missions CESAR, MARSEXPRESS, VENUS EXPRESS and HERSCHEL established and managed by the European Space Agency (ESA). He is responsible for the Pointing Unit MERTIS/BEPI COLOMBO ESA mission and a few not space projects dedicated remote sensing sensors. His is author approximately 40 scientific and technical papers